

Porous Amorphous Si Film Anodes for All-Solid-State Li Batteries

Narumi Ohta, Junichi Sakabe, Tsuyoshi Ohnishi, Kazunori Takada

National Institute for Materials Science, 1-1 Namiki, Tsukuba, Ibaraki 305-0044, Japan

E-mail: OHTA.Narumi@nims.go.jp

Some thiophosphate-based solid electrolytes exhibit high levels of resistance against electrochemical reduction leading to solid–electrolyte interphase (SEI) layer formation [1] and relatively low elastic moduli, as well as large plastic deformation capacities [2]. These are advantageous for the application of high-capacity but severe-volume-change Si electrodes (operating voltage of ~ 0.4 V vs. Li^+/Li) as the anodes in all-solid-state Li batteries. In fact, we showed that amorphous Si film anodes exhibit high capacity and good cyclability in the solid electrolyte [3–5]; however, the excellent cycling performances were only observed for the films with a thickness of <0.3 μm and an areal capacity of <0.2 mAh cm^{-2} . In this study, we attempt to overcome the limitations and increase the areal capacity to practical levels ($2\text{--}4$ mAh cm^{-2}) by using a porous Si structure. We synthesized porous amorphous Si films by the sputtering deposition method, using He as the deposition gas [6], and investigated the influence of nanometer-sized pores in the films on their cycling performance in the solid electrolyte. The resulting films showed homogeneously distributed pores (10–50 nm in size) separated by 10-nm-thick walls (Fig. 1b). The investigation reveals that introducing pores into amorphous Si anodes enhances the cycling performance in solid-state batteries owing to the porous character, which strengthens the structural integrity of the amorphous Si anodes. For instance, a porous amorphous Si film delivering an areal capacity of 2.3 mAh cm^{-2} exhibits a very low capacity fading rate of 0.06% per cycle and high coulombic efficiencies exceeding 99.8% (Fig. 2).

References:

- [1] A. Hayashi, S. Hama, F. Mizuno, K. Tadanaga, T. Minami, M. Tatsumisago, *Solid State Ionics* 175 (2004) 683–686.
- [2] A. Sakuda, A. Hayashi, M. Tatsumisago, *Sci. Rep.* 3 (2013) 2261.
- [3] R.B. Cervera, N. Suzuki, T. Ohnishi, M. Osada, K. Mitsuishi, T. Kambara, K. Takada, *Energy Environ. Sci.* 7 (2014) 662–666.
- [4] R. Miyazaki, N. Ohta, T. Ohnishi, I. Sakaguchi, K. Takada, *J. Power Sources* 272 (2014) 541–545.
- [5] R. Miyazaki, N. Ohta, T. Ohnishi, K. Takada, *J. Power Sources* 329 (2016) 41–49.
- [6] V. Godinho, J. Caballero-Hernández, D. Jamon, T.C. Rojas, R. Schierholz, J. García-López, F.J. Ferrer, A. Fernández, *Nanotechnology* 24 (2013) 275604.

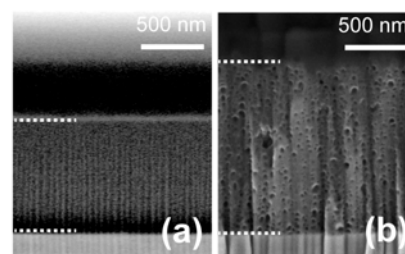


Fig. 1. SEM cross-sectional images of (a) non-porous and (b) porous films. The images were obtained at a tilt angle of 60° ; scale bars in the images are only applicable to the horizontal direction. The upper and lower dashed white lines in the images indicate the surface of amorphous Si films and stainless-steel substrates, respectively.

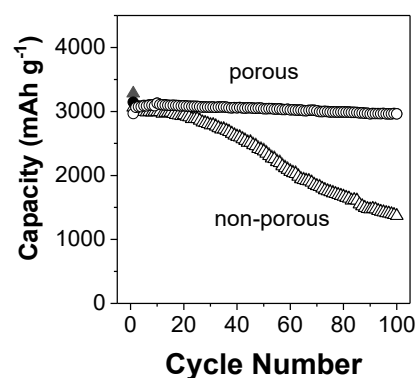


Fig. 2. Charging and discharging capacities plotted against the cycle number. The filled and empty circles indicate the charging and discharging capacities, respectively; the triangles and circles represent the results for non-porous and porous Si films, respectively. The areal mass loadings of the as-prepared non-porous and porous films were 0.70 and 0.74 mg cm^{-2} , respectively, and the thickness were 3.0 and 4.7 μm , respectively.